TSSA in inclusive production of higher-lying states of charmonium at the NICA

A. V. Karpishkov[1,2], V. A. Saleev[1,2]

[1] Samara National Research University
[2] Joint Institute for Nuclear Research

22.01.2025
SPD Physics and MC meeting

Generalized Parton Model (GPM) and it's application to calculation of TSSA

Factorization formula for the GPM

Within the GPM we can write the following expression for the differential cross-section of $2 \to 1$ hard subprocess $g(q_1) + g(q_2) \to \mathcal{C}(k)$:

$$d\sigma(pp \to \mathcal{C}X) = \int dx_1 \int d^2\mathbf{q_{1T}} \int dx_2 \int d^2\mathbf{q_{2T}} \times \times F_g(x_1, q_{1T}, \mu_F) F_g(x_2, q_{2T}, \mu_F) d\hat{\sigma}(gg \to \mathcal{C}), \quad (1)$$

where $\mathcal{C} = J/\psi, \psi(2S)$ or $\chi_c(1P)$, and

$$d\hat{\sigma}(gg \to \mathcal{C}) = (2\pi)^4 \delta^{(4)}(q_1 + q_2 - k) \frac{\overline{|M(gg \to \mathcal{C})|^2}}{2x_1x_2s} \frac{d^4k}{(2\pi)^3} \delta_+(k^2 - m_{\mathcal{C}}^2). \quad (2)$$

In a case of $2 \to 2$ subprocess $g(q_1) + g(q_2) \to \mathcal{C}(k) + g(q_3)$, $\mathcal{C} = J/\psi, \psi(2S)$ in formula (1) $d\hat{\sigma}(gg \to \mathcal{C})$ must be replaced by:

$$d\hat{\sigma}(gg \to \mathcal{C}g) = (2\pi)^4 \delta^{(4)}(q_1 + q_2 - k - q_3) \frac{\overline{|M(gg \to \mathcal{C}g)|^2}}{2x_1x_2s} \frac{d^3k}{(2\pi)^3 2k_0} \frac{d^4q_3}{(2\pi)^3} \delta_+(q_3^2). \quad (3)$$

$$q_1^\mu = \left(x_1 \frac{\sqrt{s}}{2} + \frac{\mathbf{q}_{1T}^2}{2\sqrt{s}x_1}, \mathbf{q}_{1T}, x_1 \frac{\sqrt{s}}{2} - \frac{\mathbf{q}_{1T}^2}{2\sqrt{s}x_1} \right)^\mu, \quad (4)$$

$$q_2^\mu = \left(x_2 \frac{\sqrt{s}}{2} + \frac{\mathbf{q}_{2T}^2}{2\sqrt{s}x_2}, \mathbf{q}_{2T}, -x_2 \frac{\sqrt{s}}{2} + \frac{\mathbf{q}_{2T}^2}{2\sqrt{s}x_2} \right)^\mu. \quad (5)$$

Transverse Single Spin Asymmetry (TSSA)

In inclusive process $p^{\uparrow}p \to \mathcal{C}X$ $\mathcal{C} = J/\psi, \chi_c, \psi(2S))$ TSSA is defined as:

$$A_N = \frac{d\sigma^{\uparrow} - d\sigma^{\downarrow}}{d\sigma^{\uparrow} + d\sigma^{\downarrow}} = \frac{d\Delta\sigma}{2d\sigma}. \tag{6}$$

The numerator and denominator of A_N have the form:

$$d\sigma \propto \int dx_1 \int d^2q_{1T} \int dx_2 \int d^2q_{2T} F_g(x_1, q_{1T}, \mu_F) F_g(x_2, q_{2T}, \mu_F) d\hat{\sigma}(gg \to \mathcal{C}X), \tag{7}$$

$$d\Delta\sigma \propto \int dx_1 \int d^2q_{1T} \int dx_2 \int d^2q_{2T} [\hat{F}_g^{\uparrow}(x_1, \mathbf{q}_{1T}, \mu_F) - \hat{F}_g^{\downarrow}(x_1, \mathbf{q}_{1T}, \mu_F)] \times F_g(x_2, q_{2T}, \mu_F) d\hat{\sigma}(gg \to \mathcal{C}X), \tag{8}$$

where $\hat{F}_g^{\uparrow,\downarrow}(x, q_T, \mu_F)$ is the distribution of unpolarized gluon (or quark) in polarized proton, $\hat{F}_g^{(\uparrow)}(x_1, \mathbf{q}_{1T}, \mu_F) - \hat{F}_g^{(\downarrow)}(x_1, \mathbf{q}_{1T}, \mu_F) \equiv \Delta\hat{F}_g^{\uparrow}(x_1, \mathbf{q}_{1T}, \mu_F)$ – the gluon Sivers function (GSF).

TSSA within the CGI-GPM framework

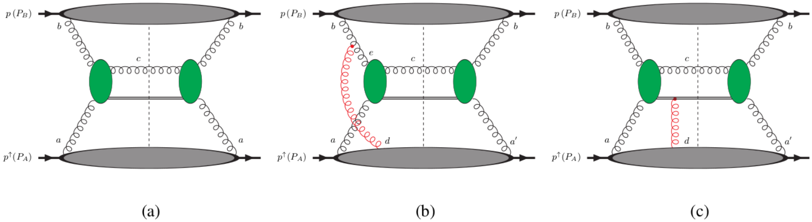

Figure 1: LO diagrams for the process $p^\uparrow p \to J/\psi X$, assuming a color-singlet production mechanism, within the GPM (a) and the CGI-GPM (b), (c). It turns out that only initial state interactions depicted in (b) contribute to the TSSA. Figure is from [D'Alesio *et.al.*, Phys. Rev. D **96**, 036011 (2017)].

In GPM (Fig. 1 (a)) we can write the numerator of the asymmetry as follows:

$$d\Delta\sigma \propto \Delta\hat{F}_g^\uparrow(x_1, \mathbf{q}_{1T}, \mu_F) \otimes F_g(x_2, q_{2T}, \mu_F) \otimes H^U_{gg\to cd}, \tag{9}$$

where $H^U_{gg\to cd} = \overline{|M(gg \to cd)|^2}$.

TSSA within the CGI-GPM framework

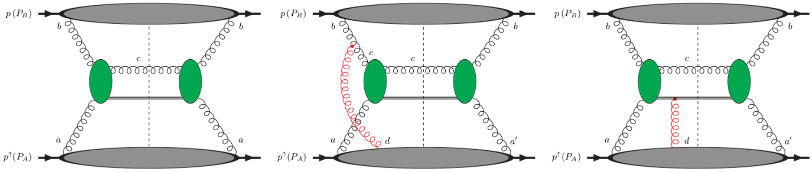

Figure 2: LO diagrams for the process $p^\uparrow p \to J/\psi X$, assuming a color-singlet production mechanism, within the GPM (a) and the CGI-GPM (b), (c). It turns out that only initial state interactions depicted in (b) contribute to the TSSA. Figure is from [D'Alesio *et.al.*, Phys. Rev. D **96**, 036011 (2017)].

Formally, the numerator of the asymmetry in the CGI-GPM approach ([L. Gamberg and Z. B. Kang, Phys. Lett. B **696**, 109 (2011)]) can be obtained from eq. (9) by with the substitution:

$$F_{1T}^{\perp g} H^U_{gg\to J/\psi g} \to \frac{C_I^{(f)} + C_{F_c}^{(f)}}{C_U} F_{1T}^{\perp g(f)} H^U_{gg\to J/\psi g} + \frac{C_I^{(d)} + C_{F_c}^{(d)}}{C_U} F_{1T}^{\perp g(d)} H^U_{gg\to J/\psi g} \equiv$$
$$\equiv F_{1T}^{\perp g(f)} H^{Inc(f)}_{gg\to J/\psi g} + F_{1T}^{\perp g(d)} H^{Inc(d)}_{gg\to J/\psi g}. \quad (10)$$

TSSA in charmonium production at NICA

TSSA of χ_{c0} at NICA (D'Alesio), $|y| \leq 3$, $\sqrt{s} = 24$ GeV.

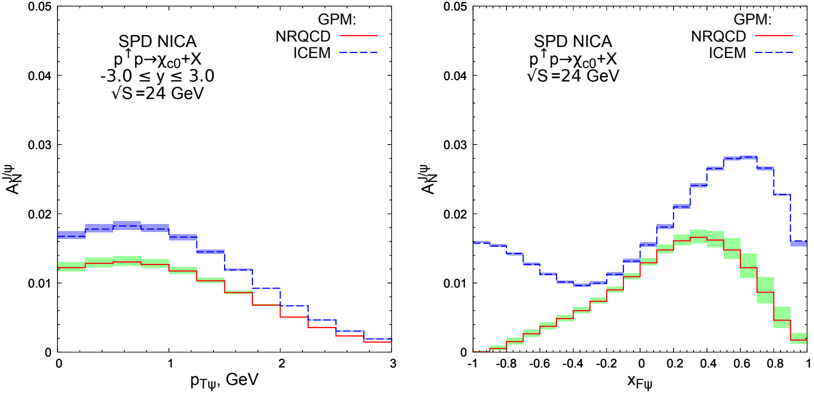

Figure 3: Predictions for TSSA $A_N^{\chi_{c0}}$ as function of p_T and x_F at $\sqrt{s} = 24$ GeV within NRQCD (solid histogram) and ICEM (dashed histogram) approaches. The D'Alesio *et al.* parametrisation of GSFs is used.

TSSA of χ_{c_0} at NICA (SIDIS1), $|y| \leq 3$, $\sqrt{s} = 24$ GeV.

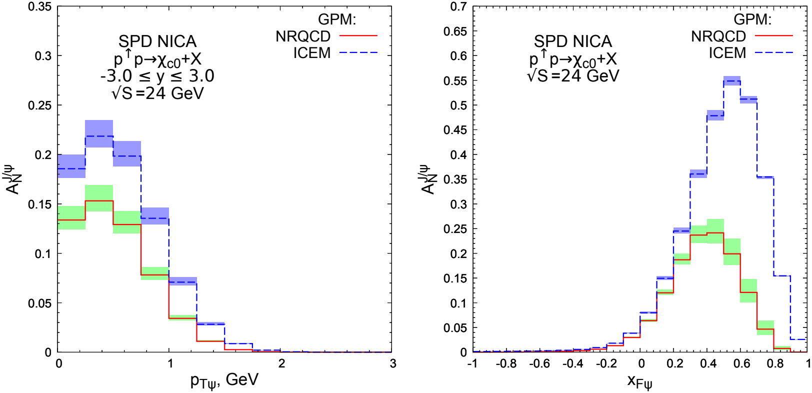

Figure 4: Predictions for TSSA $A_N^{\chi_{c0}}$ as function of p_T and x_F at $\sqrt{s} = 24$ GeV within NRQCD (solid histogram) and ICEM (dashed histogram) approaches. The SIDIS1 *et al.* parametrisation of GSFs is used.

TSSA of χ_{c_0} at NICA (SIDIS2), $|y| \leq 3$, $\sqrt{s} = 24$ GeV.

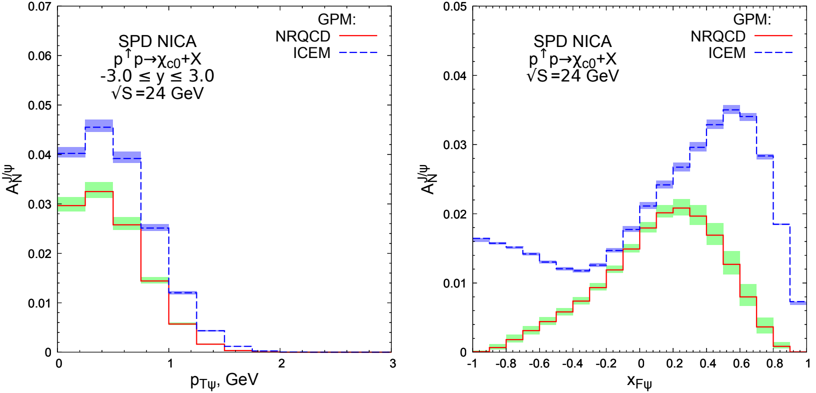

Figure 5: Predictions for TSSA $A_N^{\chi_{c0}}$ as function of p_T and x_F at $\sqrt{s} = 24$ GeV within NRQCD (solid histogram) and ICEM (dashed histogram) approaches. The SIDIS2 *et al.* parametrisation of GSFs is used.

TSSA of χ_{c_2} at NICA (D'Alesio), $|y| \leq 3$, $\sqrt{s} = 24$ GeV.

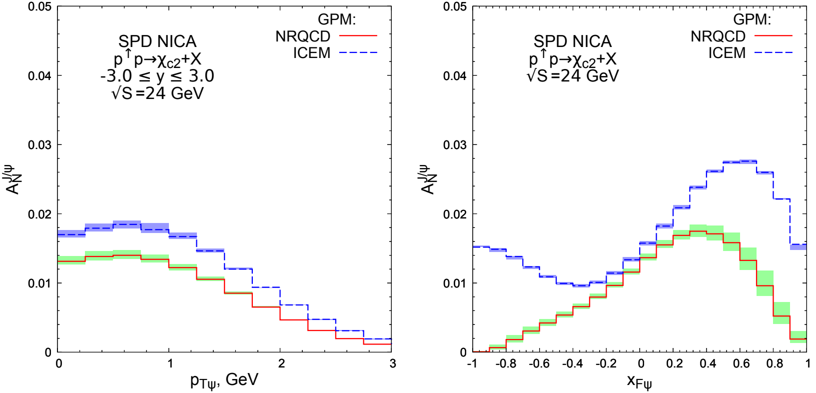

Figure 6: Predictions for TSSA $A_N^{\chi_{c2}}$ as function of p_T and x_F at $\sqrt{s} = 24$ GeV within NRQCD (solid histogram) and ICEM (dashed histogram) approaches. The D'Alesio *et al.* parametrisation of GSFs is used.

TSSA of χ_{c_2} at NICA (SIDIS1), $|y| \leq 3$, $\sqrt{s} = 24$ GeV.

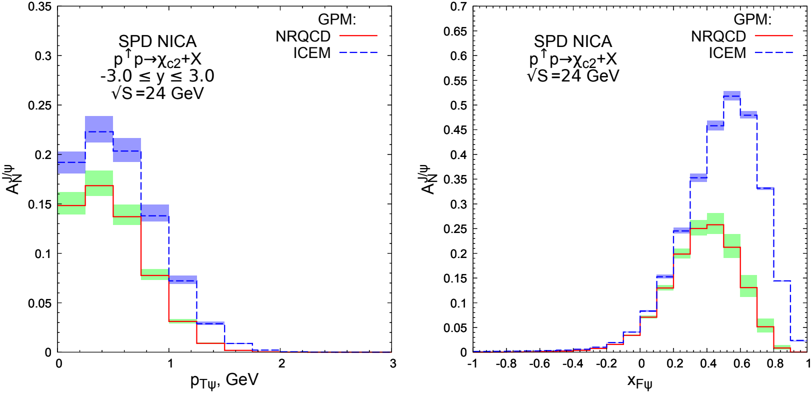

Figure 7: Predictions for TSSA $A_N^{\chi_{c2}}$ as function of p_T and x_F at $\sqrt{s} = 24$ GeV within NRQCD (solid histogram) and ICEM (dashed histogram) approaches. The SIDIS1 *et al.* parametrisation of GSFs is used.

TSSA of χ_{c_2} at NICA (SIDIS2), $|y| \leq 3$, $\sqrt{s} = 24$ GeV.

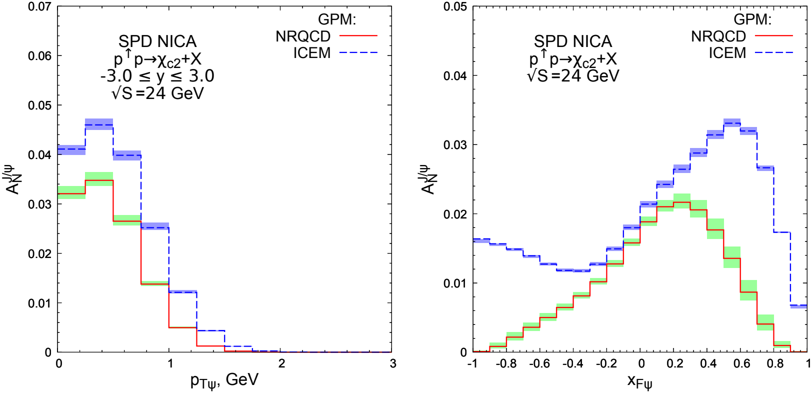

Figure 8: Predictions for TSSA $A_N^{\chi_{c2}}$ as function of p_T and x_F at $\sqrt{s} = 24$ GeV within NRQCD (solid histogram) and ICEM (dashed histogram) approaches. The SIDIS2 *et al.* parametrisation of GSFs is used.

TSSA of $\psi(2S)$ at NICA (D'Alesio), $|y| \leq 3$, $\sqrt{s} = 24$ GeV.

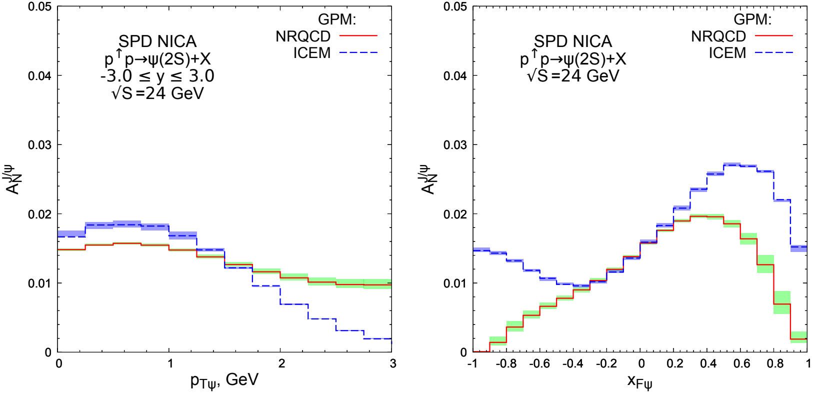

Figure 9: Predictions for TSSA $A_N^{\psi(2S)}$ as function of p_T and x_F at $\sqrt{s} = 24$ GeV within NRQCD (solid histogram) and ICEM (dashed histogram) approaches. The D'Alesio *et al.* parametrisation of GSFs is used.

TSSA of $\psi(2S)$ at NICA (SIDIS1), $|y| \leq 3$, $\sqrt{s} = 24$ GeV.

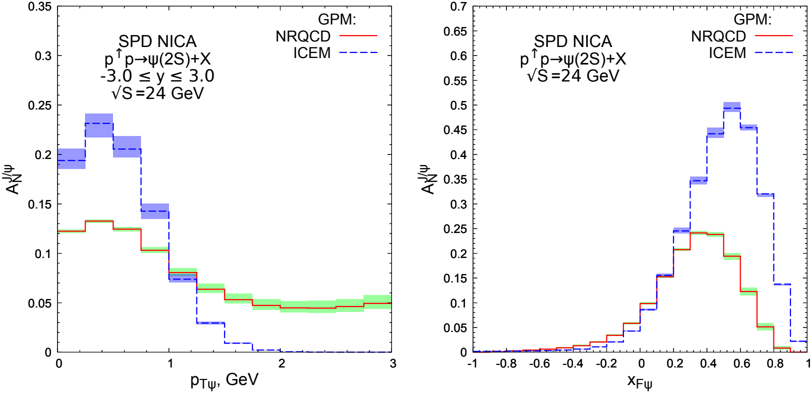

Figure 10: Predictions for TSSA $A_N^{\psi(2S)}$ as function of p_T and x_F at $\sqrt{s} = 24$ GeV within NRQCD (solid histogram) and ICEM (dashed histogram) approaches. The SIDIS1 *et al.* parametrisation of GSFs is used.

TSSA of $\psi(2S)$ at NICA (SIDIS2), $|y| \leq 3$, $\sqrt{s} = 24$ GeV.

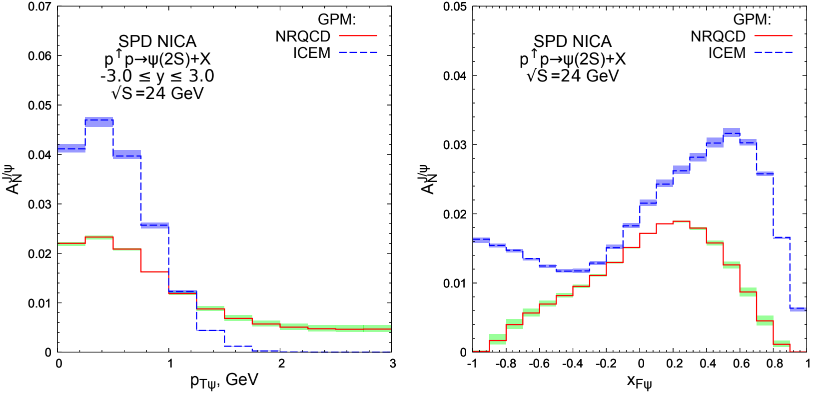

Figure 11: Predictions for TSSA $A_N^{\psi(2S)}$ as function of p_T and x_F at $\sqrt{s} = 24$ GeV within NRQCD (solid histogram) and ICEM (dashed histogram) approaches. The SIDIS2 *et al.* parametrisation of GSFs is used.

TSSA of χ_{c_1} at NICA, $|y| \leq 3$, $\sqrt{s} = 24$ GeV.

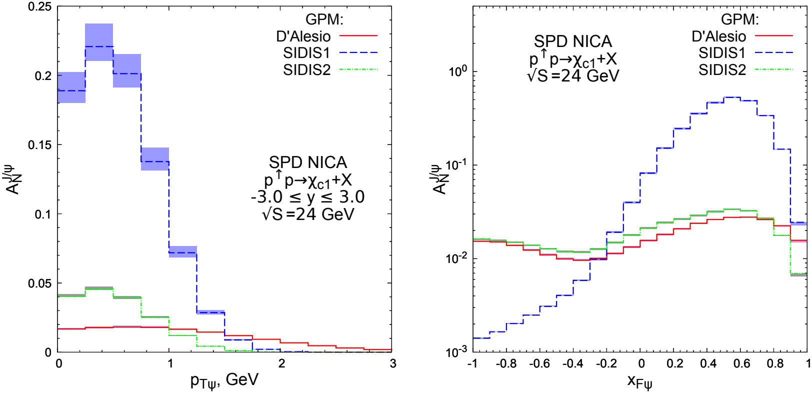

Figure 12: Predictions for TSSA $A_N^{\chi_{c1}}$ as function of p_T and x_F at $\sqrt{s} = 24$ GeV within ICEM approach.

TSSA in charmonium production at SpinQuest (Fermilab NM4)

Fermilab

Home | About | Science | Jobs | Contact | Phone Book

Newsroom | DUNE at LBNF | Community | Resources for

SpinQuest

About SpinQuest

- Physics of SpinQuest
- Polarized target
- Spectrometer
- Collaboration
- Presentations and publications
- Data Management Plan
- Contact us

SpinQuest at Work

Related Links

- University of Virginia SpinQuest Website
- University of Michigan Wiki (login required)

About SpinQuest

Main goal of SpinQuest

Every proton and neutron is made up of tinier particles called quarks and gluons, and we continue to explore how the quarks and gluons behave therein. Both quarks and their anti-matter cousins the anti-quarks play a role in creating protons and neutrons. The SpinQuest experiment is designed to explore a very particular aspect of proton and neutron structure: **Are the sea quarks orbiting around the spin axis of the nucleon?**

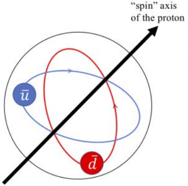

Are the anti-quarks in orbit about the spin axis of the proton?

A fixed-target experiment using the 120 GeV Main Injector beam and a polarized frozen-ammonia target.

$$\sqrt{s} = 15\ \text{GeV}, \qquad |x_F| \geq 0.4$$

TSSA of J/ψ at SpinQuest: $\sqrt{s} = 15$ GeV, $|x_F| \geq 0.4$.

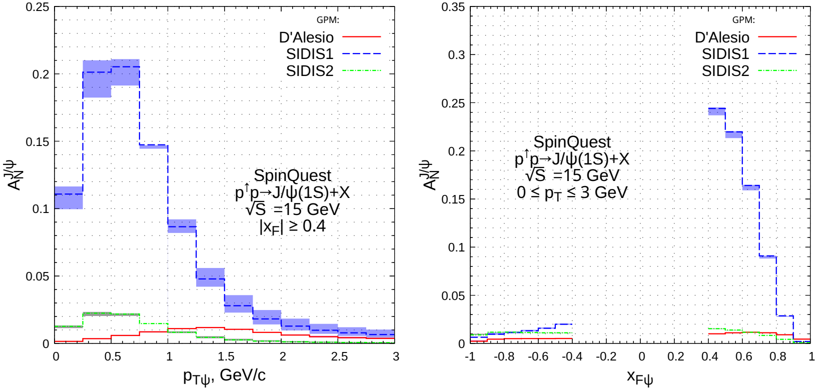

Figure 13: Predictions for TSSA $A_N^{J/\psi}$ (*prompt*) as function of p_T (left) and x_F (right) at $\sqrt{s} = 15$ GeV within GPM+CSM approaches.

Comparison to NICA: $\sqrt{s} = 27$ GeV, $|y| \leq 3$.

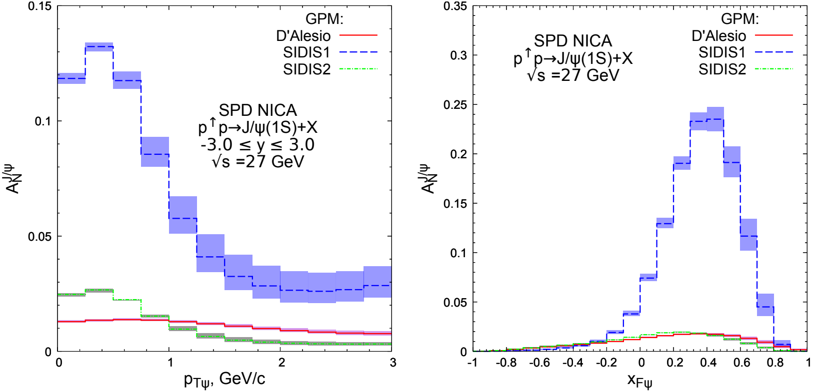

Figure 14: Predictions for TSSA $A_N^{J/\psi}$ (*prompt*) as function of p_T (left) and x_F (right) at $\sqrt{s} = 27$ GeV within GPM+CSM approaches.

TSSA of J/ψ at SpinQuest: $\sqrt{S} = 15$ GeV, $|x_F| \geq 0.4$.

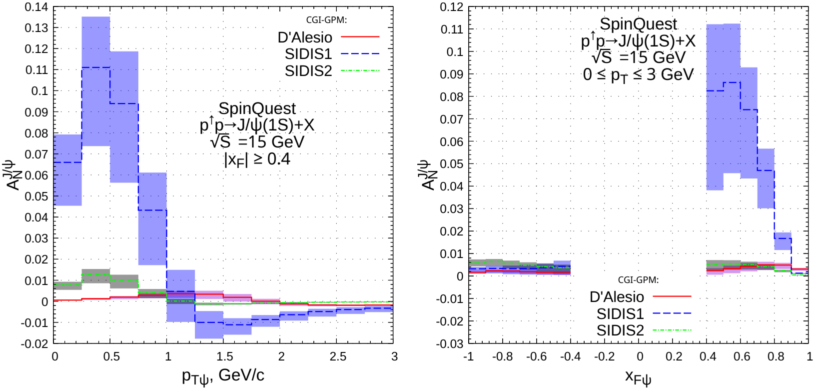

Figure 15: Predictions for TSSA $A_N^{J/\psi}$ (*prompt*) as function of p_T (left) and x_F (right) at $\sqrt{s} = 15$ GeV within CGI-GPM+CSM approaches.

A small announcement: predictions for J/ψ within Soft Gluon Resummation model.

Calculations of Kirill Shilyaev (PhD student, Samara University):

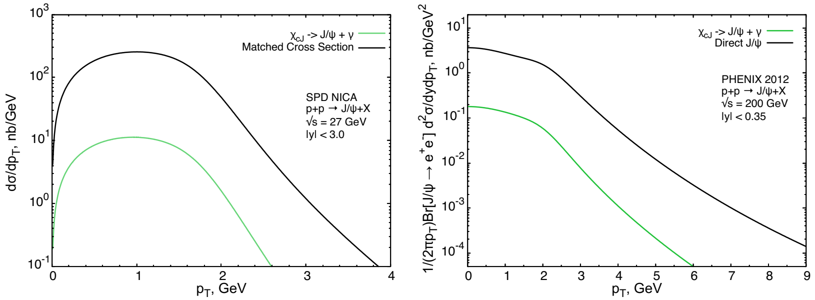

Figure 16: Predictions for cross sections for prompt J/ψ: $\dfrac{d\sigma}{dp_T}$ at NICA $\sqrt{s} = 27$ GeV (left) and $E\dfrac{d^3\sigma}{dp^3}$ at PHENIX $\sqrt{s} = 200$ GeV (right) within the SGR model.

Summary

- For all the P-wave charmonia states we see significant discrepancies between predictions within CSM and ICEM. It is especially noticeable for x_F-distribution.

Summary

- For all the P-wave charmonia states we see significant discrepancies between predictions within CSM and ICEM. It is especially noticeable for x_F-distribution.
- For $\psi(2S)$ state both p_T and x_F dependencies of A_N has big discrepancies between predictions within CSM and ICEM.

Summary

- For all the P-wave charmonia states we see significant discrepancies between predictions within CSM and ICEM. It is especially noticeable for x_F-distribution.
- For $\psi(2S)$ state both p_T and x_F dependencies of A_N has big discrepancies between predictions within CSM and ICEM.
- SIDIS1 parametrization of the GSF gives the biggest value of the TSSA.

Summary

- For all the P-wave charmonia states we see significant discrepancies between predictions within CSM and ICEM. It is especially noticeable for x_F-distribution.
- For $\psi(2S)$ state both p_T and x_F dependencies of A_N has big discrepancies between predictions within CSM and ICEM.
- SIDIS1 parametrization of the GSF gives the biggest value of the TSSA.
- At SpinQuest kinematics we see quite similar results of A_N for J/ψ.

Summary

- For all the P-wave charmonia states we see significant discrepancies between predictions within CSM and ICEM. It is especially noticeable for x_F-distribution.
- For $\psi(2S)$ state both p_T and x_F dependencies of A_N has big discrepancies between predictions within CSM and ICEM.
- SIDIS1 parametrization of the GSF gives the biggest value of the TSSA.
- At SpinQuest kinematics we see quite similar results of A_N for J/ψ.
- CGI-GPM can reproduce **negative** values of the TSSA.

Thank you for your attention!

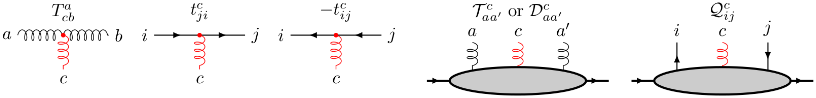

(a) (b) (c) (d) (e)

Figure 17: CGI-GPM color rules for the eikonal three-gluon (a), quark-gluon (b) and antiquark-gluon (c) vertices. The color projectors for the gluon (d) and the QSF (e) are shown as well. The eikonal gluon has color index c. Figure is from [D'Alesio *et.al.*, Phys. Rev. D **96**, 036011 (2017)].

The color factors are:

$$\mathcal{T}^c_{aa'} = \mathcal{N}_{\mathcal{T}} T^c_{aa'}, \mathcal{D}^c_{aa'} = \mathcal{N}_{\mathcal{D}} D^c_{aa'}, \mathcal{Q}^c_{ij} = \mathcal{N}_{\mathcal{Q}} t^c_{ij}, \tag{11}$$

where $T^a_{cb} \equiv -i f_{acb}$, $D^a_{bc} \equiv d_{abc}$, $\mathcal{N}_{\mathcal{T}} = \frac{1}{Tr[T^c T^c]} = 1/(N_c(N_c^2-1))$, $\mathcal{N}_{\mathcal{D}} = \frac{1}{Tr[D^c D^c]} = 1/((N_c^2-4)(N_c^2-1))$, $\mathcal{N}_{\mathcal{Q}} = \frac{1}{Tr[t^c t^c]} = 2/(N_c^2-1)$.
So, correspondingly, for the f- and d-type GSF, the relative color factor is therefore calculated from Fig. 1(b) as follows:

$$C_I^{(f)} = -\frac{1}{2} C_U, C_I^{(d)} = 0. \tag{12}$$

And in CSM of the heavy quark-antiquark pair to the FSI, depicted in Fig. 1(c):

$$C_{F_c}^{(f)} = C_{F_c}^{(d)} = 0. \tag{13}$$